EQUIVALENT VISCOUS DAMPING FOR NON-STRUCTURAL BUILDING ELEMENTS

R.J. Merino[(1)], D. Perrone[(2)], A. Filiatrault[(3)]

[(1)] *PhD student, University School for Advanced Studies IUSS Pavia, Italy, robertojavier.merinovela@iusspavia.it*

[(2)] *Research Fellow, University School for Advanced Studies IUSS Pavia, Italy, daniele.perrone@iusspavia.it*

[(3)] *Professor, University School for Advanced Studies IUSS Pavia, Italy and State University of New York at Buffalo, USA, andre.filiatrault@iusspavia.it*

Abstract

Earthquakes that have struck densely built regions during the last decades in highly populated regions have demonstrated the need for reliable methodologies to perform the seismic design of non-structural building elements that are damaged due to inertia forces arising from horizontal floor accelerations. Performance-based seismic design of non-structural elements, through a direct displacement-based design procedure, has been recently proposed to this end. This procedure is based on the concept of equivalent linearization of the response of nonlinear non-structural systems. An essential aspect of this process involves quantifying the amount of energy dissipated by a nonlinear non-structural element at its maximum expected displacement response. Energy dissipation in direct displacement-based design is usually represented through an equivalent viscous damping ratio. The first step in quantifying this parameter for some of the multitude of non-structural element typologies consists in gathering and processing experimental data that can describe the variation of the global equivalent non-structural viscous damping ratio with non-structural displacement amplitude relative to the supporting structure through an equal area approach. This first step gives not only a good estimate of the effective energy dissipated by nonlinear non-structural elements when subjected to floor acceleration time histories, but also reveals important hysteretic and mechanical properties of the same systems. In this work, some examples of test results performed on acceleration-sensitive non-structural elements available in the literature are processed in order to develop relationships between non-structural displacement relative to the supporting structure and equivalent non-structural viscous damping.

Keywords: Non-structural elements, direct displacement-based design, damping, hysteretic, equivalent linearization

1. Introduction

Damage to non-structural elements can severely compromise the overall performance of a building during and after an earthquake. Damage observed during past earthquakes [1,2] as well as loss estimation studies [3] have demonstrated that impaired non-structural elements can pose a threat to the safety of building occupants and produce catastrophic economic losses. Despite the considerable effect that non-structural elements have on the seismic performance of buildings, there is limited information on how to properly design non-structural elements to withstand earthquake ground motions. Current seismic design provisions and guidelines [4,5] prescribe procedures that are primarily based on judgment and intuition rather than on analytical or experimental results.

Many typologies of non-structural elements, such as, for example, suspended piping systems, are damaged due to excessive displacements relative to their point of support in the structure produced by inertia forces arising from horizontal floor accelerations. Non-structural elements that are damaged by floor accelerations are usually referred to as acceleration-sensitive non-structural elements and are generally designed according to equivalent static lateral force procedures [4-6]. Taking the example of suspended piping systems, their seismic design is usually achieved by installing lateral restraint systems, along the length of pipelines, which are able to resist the equivalent lateral load computed using contemporary seismic design guidelines. However, Filiatrault *et al.* [7] demonstrated that performing the seismic design of suspended piping systems using contemporary seismic design guidelines may produce un-conservative results, and, therefore, proposed a direct displacement-based procedure for non-structural elements. An illustrative example of the procedure was performed to design the lateral restrain of a suspended piping system supported on a reinforced concrete moment resisting frame located in Italy [7].

Direct displacement-based design, which was first developed for structures by Priestley *et al.* [8], relies on the assumption that a fully non-linear system can be represented by an equivalent linear system. The maximum displacement response of the equivalent linear system should be similar to the maximum displacement response of the nonlinear system. In order to achieve this equality, the equivalent linear system should be characterized by an equivalent period that is computed using the secant stiffness related to the maximum displacement response and an appropriate level of equivalent viscous damping to account for energy dissipation [9]. The total amount of energy dissipated by the non-linear system is represented by a single equivalent viscous damping ratio that varies with displacement response amplitude. One simple way to quantify the variation of equivalent viscous damping ratio with displacement amplitude is by equating the area under the complete hysteretic curve of the non-linear system with the area under the curve of an equivalent visco-elastic system, as first proposed by Jacobsen [10, 11]. This procedure, for example, was carried out in [12-15] to calibrate equations that relate displacement ductility to equivalent viscous damping in reinforced concrete structures.

Anajafi and Medina [16] reviewed experimental data on non-structural elements that have been performed to determine non-structural damping ratios over a broad range of displacement amplitudes and concluded that the available data are scarce or non-existent. Additionally, from the few studies that do exist, it is difficult to provide general considerations for use in practical purposes [17,18]. Considering that non-structural damping is crucial in estimating the seismic demand acting on non-structural elements [16,19-21], there is an urgent need to illuminate this mostly neglected field. In this paper, existing results from pseudo-static reversed cyclic tests performed recently on sway braced trapeze systems, used to restrain suspended piping systems, are processed in order to develop simplified models that relate equivalent viscous damping ratio to non-structural displacement amplitude relative to the supporting structure. The damping models are based solely on the equal area approach and can be used for preliminary direct displacement-based design and/or assessment of suspended piping systems.

2. Direct Displacement-Based Design of Non-Structural Elements

Filiatrault *et al.* [7] proposed recently a direct displacement-based design procedure that applies to acceleration sensitive non-structural elements that are supported on a single location on the structure and that are damaged due to excessive relative displacements relative to their point of support in the structure. Suspended piping systems are a good example for which the direct displacement-based design procedure can be applied to. The direct displacement-based design procedure, applied to non-structural elements, is briefly summarized in the following paragraphs and in Figure 1. Further information on the procedure is available in [7].

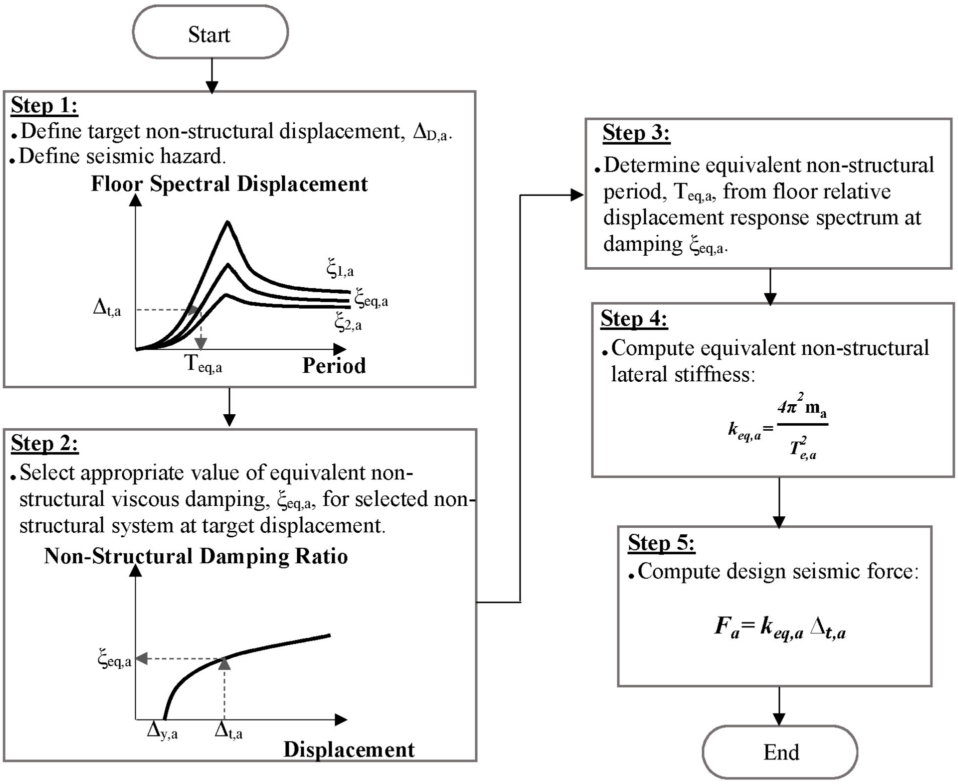

Fig. 1 – Flow-chart of direct displacement-based design of non-structural elements

The first step of the direct displacement-based design process is to define a target displacement, $\Delta_{t,a}$, that the non-structural element should not exceed under a given level of seismic hazard ground shaking. The seismic hazard associated to the target displacement, $\Delta_{t,a}$, should be defined as a relative displacement floor response spectrum. During the past several years, important efforts have been made to develop methodologies that can predict absolute acceleration floor response spectra without the need to conduct non-linear time history analyses of the supporting structure [19-21]. Once an absolute acceleration spectrum is estimated, an estimate of the corresponding relative displacement floor response spectrum can be obtained by using the pseudo-spectral relationship [21, 22].

The second step in the design process is to determine the appropriate level of equivalent viscous damping, $\xi_{eq,a}$, of the equivalent linear system. As already mentioned, the simplest way to obtain this value is by using Jacobsen's [10,11] pre-established equal area relation that can be expressed as follows:

$$\xi_{eq,a} = \frac{E_D}{2\pi F_a \Delta_{t,a}} \tag{1}$$

where E_D is the total energy dissipated by the non-linear non-structural element in one whole cycle of response, $\Delta_{t,a}$ is the maximum displacement achieved during that cycle and F_a is its corresponding force level. Note that additional energy dissipation, not related to hysteretic energy dissipation, can be accounted for by using the additional inherent damping term, $\xi_{i,a}$. Non-structural hysteretic curves obtained from a database of pseudo-static reversed cyclic tests can be used to generate $\xi_{eq,a}$-$\Delta_{t,a}$ data pairs by using Equation 1. Simple generic equations can then be developed for each non-structural element typology [14,15]. In this study, this process is shown in detail to develop a simplified damping model for suspended piping restraint trapeze installations.

The relative displacement floor response spectrum from step 1 is computed for the appropriate level of equivalent viscous damping found in step 2. Then, the third step consists in entering the relative displacement floor response spectrum using the target displacement and finding an equivalent non-structural period, $T_{eq,a}$. Using the equivalent non-structural period, $T_{eq,a}$, and the seismic weight, W_a, of the non-structural element, an equivalent non-structural stiffness, $k_{eq,a}$, can be computed (Fig. 1). Finally, the required lateral force that the non-structural element must resist in order to achieve the target displacement, $\Delta_{t,a}$, is computed as the product of the same target displacement by the equivalent non-structural stiffness, $k_{eq,a}$. Note that in the case of assessing an existing non-structural element an iterative procedure is required because the force level is known while the displacement is unknown.

3. Case Study: Development of a Damping Model for Suspended Piping Restraint Installations

3.1 Experimental Data

The first step required to develop a simplified equation that can relate an equivalent viscous damping ratio to displacement amplitude ($\xi_{eq,a}$-$\Delta_{t,a}$) for a given typology of non-structural element is to collect data from reversed cyclic loading tests performed on non-structural elements. Perrone *et al.* [23] performed reversed cyclic loading tests on four types of suspended piping restraint trapeze installations. The specimens were chosen to be representative of the most common assemblies installed in commercial and industrial buildings in Italy. As a case study, the data from two suspended piping restraint trapeze typologies tested by Perrone *et al.* are processed to develop expressions that relate equivalent viscous damping ratio to displacement amplitude. The typologies of suspended piping restraint trapeze installations referred to in this study are made by channel elements; one typology is braced in the transverse direction (Figure 2a) while the other one is braced in the longitudinal direction (Figure 2b).

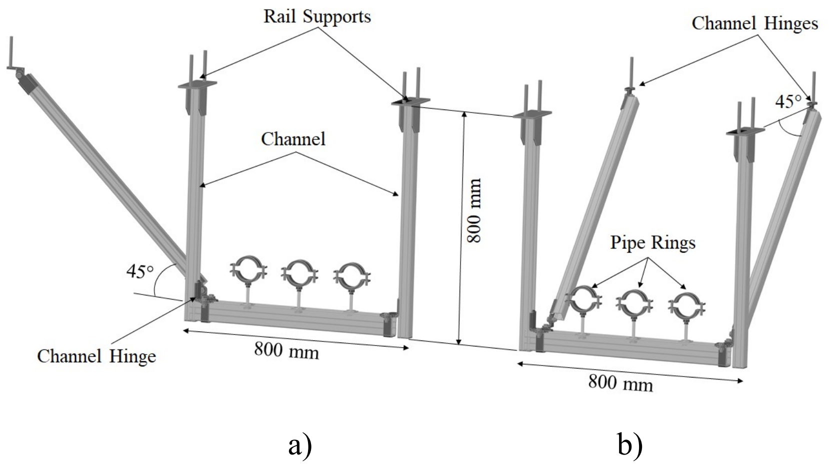

Fig. 2 – Suspended sway braced trapeze assemblies tested by Perrone *et al.* [23] with: a) transverse bracing and b) longitudinal bracing

As can be seen from Figure 2, both trapeze assemblies are constructed by a horizontal channel and two vertical channels of 800 mm in length. The cross sections of the channel elements have a square shape with a side dimension of 41 mm for all cases. The angle between the braces and the horizontal channel is 45º for both configurations. The vertical channels are connected to the horizontal channel by angles while each diagonal bracing is connected to both the horizontal channel and the ceiling slab by channel hinges. The vertical channels are connected to the ceiling slab by rail supports. Short vertical threaded rods are used to connect stiff pipe rings to the horizontal channels. The pipe rings are used to connect the pipes to the suspended piping restraint trapeze installation.

Perrone *et al.* [23] performed two reversed cyclic loading tests for each typology of suspended piping restraint trapeze installation. Each reversed cyclic test consisted on loading simultaneously two piping restraint trapeze installations mounted on a rigid frame. The two trapezes were linked by a set of four steel rigid pipes. The horizontal load was applied to the specimens by connecting an actuator to the four pipes. The FEMA 461 [24] quasi-static loading protocol was used to perform the reversed cyclic tests. The loading protocol consisted on two repeated cycles of step-wise increasing deformation amplitudes. The hysteretic force-displacement curves for the first cyclic test of both configurations are presented in Figure 3 as black lines. The longitudinally braced trapeze shows a higher peak strength and a larger displacement capacity than the transversely braced trapeze. The specimens present a highly nonlinear behavior that is the results of the yielding of the connections between the diagonal, vertical and horizontal channels. Further information on the test set-up and a more detailed discussion on the experimental results can be found in [23]. Note that the force reported in Figure 3 is the total force measured in the actuator divided by two since the test consisted of two-trapeze subassemblies tested simultaneously. Using the hysteretic force-displacement curves from the four tests, Eq. (1) can be used to compute equivalent viscous damping ratio-displacement amplitude data pairs ($\xi_{eq,a}$-$\Delta_{t,a}$).

3.2 Numerical Modelling

In order to help develop a simplified equation that can relate equivalent viscous damping to displacement amplitude, a predefined numerical hysteretic model can be fitted to the data. This is done because generalized hysteretic models are simpler to work with, and because it is an easy way to make the results more general. If the parameters used to develop the numerical models describing the hysteretic response of the tested configurations can be also applied to different configurations that would be tested in the future, then any damping-displacement equation that applies to configurations tested in this study would also apply to other configurations. The Pinching4 material model implemented in the OpenSees finite element simulation program [25] is used here to model the hysteretic cyclic behavior of the piping restraint trapeze installations. This material model consists of a piecewise linear backbone curve, a piecewise linear unload-reload path, and three damage rules that control the evolution of these paths [26].The Pinching4 material model was used to fit a mathematical model to the piping restraint trapeze installations because of its versatility; the model can capture both pinching and non-pinching behaviors and it allows for an asymmetrical backbone curve.

The shape of the backbone curve was calibrated by joining the peaks of each test cycle by a piecewise linear curve that started from the origin. This process was done separately for both the positive and negative directions. The final estimates of the backbone curve parameters, except for the force and displacement that signal the first change of slope for both the transverse and longitudinal directions, were defined as the average from the two reversed cyclic tests performed by Perrone *et al.* [23] on each sway braced trapeze assembly. All the other parameters describing the hysteretic response were calibrated using a trial and error process comparing the numerical data against the experimental data in terms of: i) force-displacement hysteretic curve, ii) absorbed energy, and iii) variation of equivalent viscous damping with displacement amplitude computed, for both the mathematical representation and the experimental data, using Eq. (1). In order to assess the effectiveness of the numerical models, the reverse cyclic tests were numerically reproduced in OpenSees [25] using a single degree of freedom model. The piping restraint installations were modelled using a zeros length translational spring to which the properties of the Pinching4 material model were assigned. The cyclic loading protocol used during the tests [24] was reproduced for the numerical simulation. Figure 3 shows the comparison between the final fit of the Pinching4 numerical models and the experimental results. The numerical models match the experimental results relatively well in terms of peak displacements and forces achieved during each cycle for both configurations.

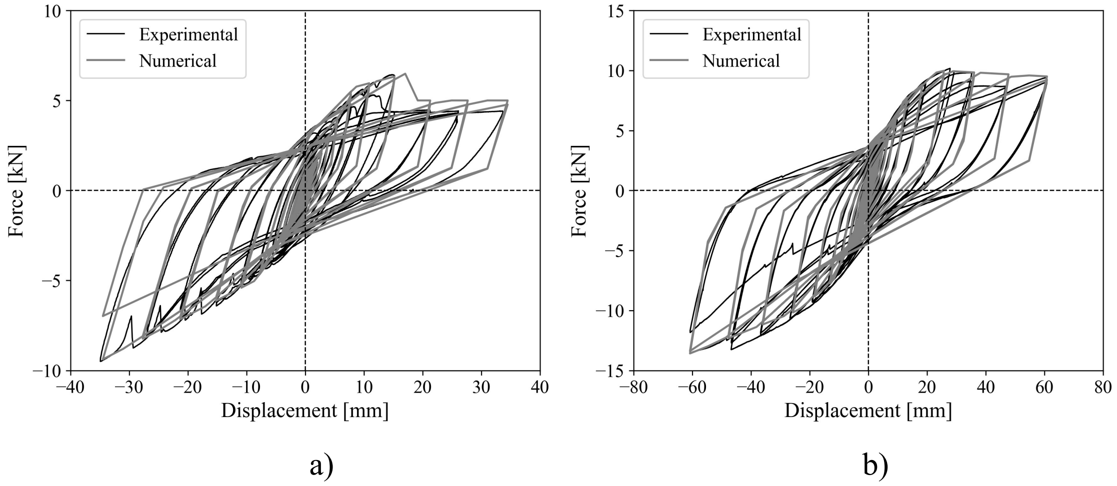

Fig. 3 – Experimental and numerical force-displacement hysteretic curves for sway braced trapezes with: a) transverse bracing and b) longitudinal bracing

Additionally, Figure 4 presents the fit of the numerical model to the experimental data in terms of absorbed energy. The absorbed energy was calculated by numerically integrating the hysteretic force-displacement curves shown in Figure 3 and then plotting it against the sequence of the points in the same curves. The absorbed energy at the i^{th} point of the hysteretic force-displacement curves is the sum of the absorbed energy at that step and at all the previous steps. Note that, in order to match, both the numerical and experimental curves should have the same proportion of points per cycle. The experimental curves are shown as black lines, with the first test plotted with a continuous line and the second test plotted with a dashed line. The results from the numerical model are plotted in grey.

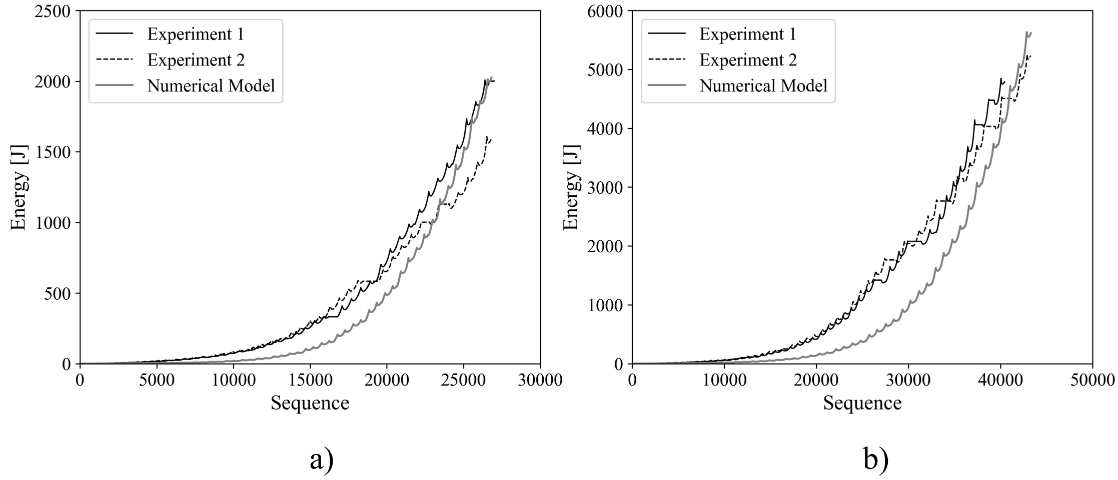

Fig. 4 – Experimental and numerical absorbed energy curves for sway braced trapezes with: a) transverse bracing and b) longitudinal bracing

The curves plotted in Figure 4 show that, in terms of absorbed energy, the proposed numerical model gives a relatively good estimate of the experimental energy absorbed. However, a lower absorbed energy for the initial cycles characterized by small displacements can be observed from the numerical model. Nevertheless, the total amount of absorbed energy is well capture by the numerical model. This behavior can be observed for both transverse and longitudinal bracing directions. It is worth noting that the obtained results can be considered conservative since the numerical model tends to dissipate less energy than the one observed during the reversed cyclic tests. A cycle-by-cycle analysis of both trapeze typologies revealed that the numerical model tends to underpredict the size (fatness) of the hysteretic loop at low displacement amplitudes while it over predicts it at larger displacements. This explains the shape of the absobed energy curves shown in Figure 4.

Finally, Figure 5 compares the results of equivalent viscous damping plotted against displacement amplitude, obtained using Eq. (1), from both cyclic tests (black dots) and from the numerical simulation (grey dots). Similar trends to the absorbed energy are observed in terms of equivalent viscous damping ratio. In general, the experimental equivalent viscous damping ratio starts to increase rapidly as soon as deformations are imposed to the piping restaint trapeze installations. This rapid increase in equivalent viscous damping demonstrates that these systems tend to behave nonlinearlly (they unload and relaod through different paths) from very low displacement amplitudes. The two tested configurations do not show a clearly defined elastic range of response. For this reason, the first point of the backbone curve, which denotes the point when the system starts to dissipate energy by forming hysteretic loops, was calibrated using a trial and error procedure as with the other cyclic parameters. Further, at a given level of displacement amplitude, the equivalent viscous damping ratio becomes basically constant (at around 20% of critical). The transverse piping restraint trapezes show a slightly higher level of equivalent viscous damping than the longitudinal ones. The numerical model shows the same trends as the experimental data although it tends to be conservative (underpredicts the level of equivalent viscous damping) at displacement amplitudes from 2.0 mm to 10.0 mm for the transverse sway braced trapezes, and from 5.0 mm to 15.0 mm for the longitudinal sway braced trapezes.

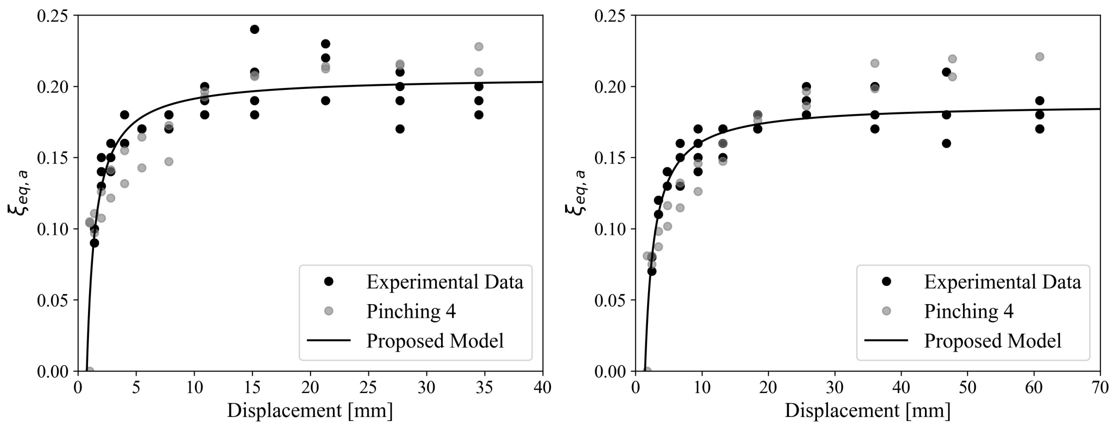

a) b)

Fig. 5 –Variation of experimental and numerically-predicted equivalent viscous damping ratio with displacement amplitude for sway braced trapezes with a) transverse bracing and b) longitudinal bracing

For sake of completeness and for ease of reproduction, the parameters of the optimized Pinching4 material model for both sway braced trapeze typologies are presented in Table 1.

Table 1 – Parameters for the Pinching4 material model

Backbone	**ePf1 [kN]**	**ePf2 [kN]**	**ePf3 [kN]**	**ePf4 [kN]**	**ePd1 [mm]**	**ePd2 [mm]**	**ePd3 [mm]**	**ePd4 [mm]**
Transverse	0.5	5.75	6.5	5.0	0.09	8.5	17.2	17.25
Longitudinal	0.6	7.5	10.0	9.5	0.1	12.0	24.0	61.0

Backbone cont.	**eNf1 [kN]**	**eNf2 [kN]**	**eNf3 [kN]**	**eNf4 [kN]**	**eNd1 [mm]**	**eNd2 [mm]**	**eNd3 [mm]**	**eNd4 [mm]**
Transverse	-0.25	-5.0	-9.5	-7.5	-0.09	-8.5	-35.2	-36.1
Longitudinal	-0.6	-7.5	-10.0	-13.5	-0.1	-12.0	-24.0	-60.0
Cyclic	**rDP**	**rFP**	**uFP**	**rDN**	**rFN**	**uFN**	**gK1**	**gK2**
Transverse	0.1	0.55	0.0	0.15	0.35	-0.15	0.7	0.0
Longitudinal	0.1	0.45	-0.2	0.4	0.55	-0.2	0.75	0.0
Cyclic cont.	**gK3**	**gK4**	**gKL**	**gD1**	**gD2**	**gD3**	**gD4**	**gDL**
Transverse	0.0	0.0	0.6	0.7	0.0	0.0	0.6	0.1
Longitudinal	0.0	0.6	0.75	0.7	0.0	0.0	0.6	0.05

Note that the force degradation parameters, not shown in Table 1, were assumed to be zero for both trapeze configurations.

3.3 Simplified Damping Model

A simplified damping model was fitted to the equivalent viscous damping-displacement amplitude data pairs ($\xi_{eq,a}$-$\Delta_{t,a}$) computed from the experimental results presented in Section 3 and plotted in Figure 5 as black dots. A first attempt was made by deriving the theoretical area of the Pinching4 material model dependent on the parameters shown in Table 1. This exercise was also performed by Dwairi *et al.* [9] for the bilinear elastic-plastic with hardening, flag shape, Takeda thin, and Takeda fat hysteretic models. Unfortunately, since the Pinching4 material model depends on many parameters (37 parameters in total), and since it is not symmetric for both directions of loading, the resulting equation, relating equivalent viscous damping with displacement amplitude derived using Eq. (1), is extremely long and cumbersome to use, making it practically impossible to be used in practice.

An alternative practical option to fit an equation relating equivalent viscous damping ratio and displacement amplitude for the two typologies of piping restraint trapeze installations would be to fit a simple bilinear model to the experimental data. This process has been followed by various researchers in the past [9,13] to fit simplified damping equations for structural systems. The form of the equation relating equivalent viscous damping to displacement amplitude for a simple bilinear model, derived using Eq. (1), can be expressed as follows:

$$\xi_{eq,a} = \frac{C}{\pi}\left(1 - \frac{\Delta_{y,a}}{\Delta_{t,a}}\right) \tag{2}$$

where $\xi_{eq,a}$ is the equivalent viscous damping ratio of the non-structural element, $\Delta_{t,a}$ is the displacement amplitude of the non-structural element, $\Delta_{y,a}$ is the yield displacement of the non-structural element, and C is a constant to be fitted to the data. The constant C is controlled by the fatness of the hysteresis loops. A value of C equal to 2 denotes an elastic perfectly plastic system. Note that the hysteresis loops predicted by the numerical Pinching4 material model, shown in Figure 3 exhibit, approximately, the shape of an inclined parallelogram. This shape is consistent with a thinner bilinear system as the one implied by Eq. (2). A bilinear system for which $C < 2$ can be considered a thin bilinear system.

Further to fitting the value of the constant C to the data, in this work, the value of the yield displacement, $\Delta_{y,a}$, was also determined from fitting Eq. (2) to the experimental data. The reasons behind this are that the piping restraint trapeze installations studied in this work, show important levels of energy dissipation even for very small displacement amplitudes. In fact, the force and displacement values of the first point on the backbone curve of the Pinching4 numerical models, in the positive and negative directions, were calibrated as cyclic parameters, using the trial and error methodology described in Section 4, in order to capture the substantial energy dissipation of these systems at small displacement amplitudes. In contrast, Perrone *et al.* [23] defined simple response parameters for the tested piping restraint trapeze installations using the FEMA P-795 guidelines [27]. The yield displacement of the systems was defined by passing a line that goes from the origin to the secant to 40% of the ultimate strength of the system, and then intersects a horizontal line defined by the ultimate strength of the system. The average values of yield displacements reported by Perrone *et al.* are 13.1 mm and 17.3 mm for the transverse and longitudinal piping restraint trapezes respectively. By comparing these values with the results from Figure 3, it can be observed that they clearly denote the displacement at which the ultimate force capacity is, approximately, reached, but they do not denote the displacement at which hysteretic energy dissipation starts to increase significantly. As already discussed in Section 4, these systems do not show a clearly defined elastic branch. Usually, in structural systems, the point where the maximum force capacity is achieved, more or less, coincides with the point where significant levels of hysteretic energy dissipation start to occur [8]. This does not occur with this typology of piping restraint trapeze installations. These systems start to dissipate considerable amounts of hysteretic energy at displacements that are much lower than the yield displacement. Therefore, for the purpose of this work, the yield displacement defined in Eq. (2) is referred to as the displacement that activates the nonlinear behavior, or activation displacement, $\Delta_{a,a}$, and it differs from the yield displacement calculated according to FEMA P-795 [27].

Equation 2 is fitted to the experimental equivalent viscous damping ratio-displacement amplitude data pairs ($\xi_{eq,a}$-$\Delta_{t,a}$), black dots in Figure 5, by minimizing the sum of the squared errors between the equation and the data. A trial and error approach was used by varying both C and $\Delta_{a,a}$ through a broad range of possible values and computing the sum of the squared errors. Equations (3) and (4) report the values of C and $\Delta_{a,a}$ that produced the minimum squared error between the data and Eq. (2), for both transverse and longitudinal directions respectively:

$$\xi_{eq,a} = \frac{0.65}{\pi}\left(1 - \frac{0.76}{\Delta_{t,a}}\right) \qquad for\ \Delta_{t,a} > 0.76mm \tag{3}$$

$$\xi_{eq,a} = \frac{0.59}{\pi}\left(1 - \frac{1.42}{\Delta_{t,a}}\right) \qquad for\ \Delta_{t,a} > 1.42mm \tag{4}$$

where $\Delta_{t,a}$ is in mm. Note that Eq. (3) applies for transversely braced piping restraint trapeze systems and Eq. (4) applies for longitudinally braced piping restraint trapeze systems. Both Eq. (3) and Eq. (4) are plotted as black lines in Figures 5a and 5b respectively alongside the experimental and numerical data. The coefficient of determination, R^2, was computed for both simplified equations in order to determine how well they fit the numerical data. The value of R^2 between Eq. (3) and the experimental data for the transversely braced trapezes is equal to 0.74. The value of R^2, meanwhile, between Eq. (4) and the experimental data for the longitudinally braced trapezes is 0.89. These values of R^2 demonstrate a good match between the proposed simplified equations and the experimental data from reversed cyclic tests of piping restraint trapeze systems.

Comparisons of the behavior of transverse and longitudinal piping restraint trapezes can be made by analyzing the final forms of Equations (3) and (4). Namely, the value of C for the transversely braced trapezes is slightly higher than that for the longitudinally braced trapezes. This implies that transversely braced piping restraint trapezes have a fatter hysteretic loop than their longitudinally braced counterparts and, therefore, dissipate higher amounts of energy at the same displacement amplitude and, in general, develop higher values of equivalent viscous damping. Note that the longitudinally braced trapezes have higher ultimate strength and displacement capacity, and therefore, absorb more total energy than the transversely braced trapezes (Figure 4). The value of the activation displacement, $\Delta_{a,a}$, is also lower for the transversely braced trapezes than for the longitudinally braced trapezes. This implies that the transversely braced trapezes start to dissipate energy at smaller displacement amplitudes than the longitudinally braced trapezes. The nonlinear mechanisms in the former systems are engaged for smaller displacement amplitudes. The difference in the dissipative behavior between transversely and longitudinally braced piping restraint trapezes is probably due to the fact that the transversely braced trapezes incorporates only a single brace, while the longitudinally braced trapezes ones have two braces, forcing the former to place higher force and deformation demands on the connections between channel elements, which are the main source of nonlinearity of these systems.

4. Conclusions

The seismic design and assessment of non-structural building elements using a direct displacement-based procedure requires the definition of the relationship between equivalent viscous damping ratio and displacement amplitude for specific non-structural typologies. In this work, data from an experimental campaign on suspended piping restraint trapeze installations was used to develop two simplified equations relating non-structural equivalent viscous damping ratio with displacement amplitude relative to the supporting structure. The equations were developed for two channel piping restraint trapeze installations, the first one braced in the transverse direction while the second one braced in the longitudinal direction. The main findings of the study are listed below:

1. Channel piping restraint trapeze installations have a highly nonlinear hysteretic behaviour starting from very small displacement amplitudes. A clearly defined elastic branch cannot be defined for these systems. The displacement value at which equivalent viscous damping starts to increase substantially is different from the nominal yield displacement of the system. Equivalent viscous damping ratios as high as 20% were observed for large displacement amplitudes.
2. The Pinching4 numerical hysteretic material model, available in OpenSees, was fitted to the experimental data. The numerical model was an intermediate step in developing a simplified equation relating equivalent non-structural viscous damping and displacement. The numerical model helped to reveal a simplified way to approximate the shape of the hysteresis loops obtained from the cyclic tests.
3. Simplified damping equations were developed for use in direct displacement-based design and assessment of this type of non-structural elements. The models are based on a simple bilinear model with a thin shape.

Even though the equations proposed in this study are recommended for direct displacement-based design of suspended piping systems, they still require proper validation/calibration through non-linear time history dynamic analyses. It has to be verified if using the equations proposed herein for direct displacement-based design produce suspended piping systems that achieve the target displacement imposed at the start of the design process. The displacement response of the non-linear systems, represented by the numerical models, should approximate well the displacement response of the equivalent linear systems, represented by the simplified equations. The numerical models developed within this study can be used for this purpose. If necessary, correction factors would have to be applied to the proposed equations. The authors are currently conducting this validation/calibration study.

7. Acknowledgements

The work presented in this paper has been developed within the framework of the project “Dipartimenti di Eccellenza”, funded by the Italian Ministry of Education, University and Research at IUSS Pavia. The EUCENTRE Foundation is gratefully acknowledged for the provided financial support to the first author of this paper. The authors gratefully acknowledge also the Italian Department of Civil Protection (DPC) for their financial contributions to this study through the ReLUIS 2019-2021 Project (Work Package 17 - Contributi Normativi Per Elementi Non Strutturali).

8. References

[1] Perrone D, Calvi PM, Nascimbene R, Fischer E, Magliulo, G. (2018): Seismic performance and damage observation of non-structural elements during the 2016 Central Italy Earthquake. *Bulletin of Earthquake Engineering*, DOI: 10.1007/s10518-018-0361-5.

[2] Filiatrault A, Uang CM, Folz B, Christopoulos C, Gatto K (2001): Reconnaissance report of the February 28, 2001 Nisqually (Seattle-Olympia) earthquake. *Structural Systems Research Project Report No. SSRP-2000/15*, Department of Structural Engineering, University of California, San Diego, La Jolla, CA, 62 pp.

[3] O'Reilly GJ, Perrone D, Fox M, Monteiro R, Filiatrault A (2018): Seismic assessment and loss estimation of existing school buildings in Italy. *Engineering Structures,* **168**(1), 142-162.

[4] ASCE (2016): *ASCE 7-16: Minimum design loads for buildings and other structures*. American Society of Civil Engineers, Reston, Virginia, USA, 889 p.

[5] CEN (2004): *EN-1998-1:2004: E: Eurocode 8 – Design provisions for earthquake resistant structures*. Comité Européen de Normalization, Brussels, Belgium.

[6] FEMA (2012): *Reducing the risks of nonstructural earthquake damage – a practical guide*. FEMA E-74, Federal Emergency Management Agency, Washington, DC, USA.

[7] Filiatrault A, Perrone D, Merino RJ, Calvi GM (2018): Performance-based seismic design of non-structural building elements. *Journal of Earthquake Engineering*, DOI: 10.1080/13632469.2018.1512910.

[8] Priestley MJN, Calvi GM, Kowalsky MJ. (2007): Displacement-Based Seismic Design of Structures, *IUSS Press*, Istituto Universitario di Studi Superiori di Pavia, Pavia, Italy.

[9] Dwairi HM, Kowalsky MJ, Nau JM (2007): Equivalent damping in support of Direct Displacement-Based design, *Journal of Earthquake Engineering,* **11**(4):512-530.

[10] Jacobsen LS (1930): Steady forced vibrations as influenced by damping. *ASME Transactions*, American Society of Mechanical Engineers, **52**(1), 169-181.

[11] Jacobsen LS (1960): Damping in composite structures. *2nd World Conference in Earthquake Engineering*, Vol. 2, Tokyo and Kyoto, Japan, 1029-1044.

[12] Priestley MJN (1993): Myths and fallacies in earthquake engineering – conflicts between design and reality. *Bulletin of the New Zealand National Society for Earthquake Engineering*. **26**(3) 329-341.

[13] Priestley MJN (2003): Myths and fallacies in earthquake engineering, revisited. *The Mallet Milne Lecture*. IUSS Press. Pavia, Italy.

[14] Gulkan P, Sozen MA (1974): Inelastic Response of Reinforced Concrete Structures to Earthquake Motions. *Journal of the American Concrete Institute.* **71**, 604-610.

[15] Fardis MN, Panagiotakos TB (1996): Hysteretic damping of reinforced concrete elements. *11th World Conference on Earthquake Engineering*; Acapulco, Mexico.

[16] Anajafi H, Medina R (2019): Damping modification factor for elastic floor spectra. *Bulletin of Earthquake Engineering*. **17**, 6079-6108.

[17] Malhotra PK, Senseny PE, Braga AC, Allard RL (2003): Testing Sprinkler-Pipe Seismic-Brace Components. *Earthquake Spectra*, **19**(1), 87-109.

[18] Wood RL, Hutchinson TC, Hoehler MS, Kreidl B (2014): Experimental Characterization of Trapeze Assemblies Supporting Suspended Nonstructural Systems. *Proceedings of the 10th US National Conference on Earthquake Engineering*, *Paper No. 905*; Anchorage, Alaska, pp. 10.

[19] Sullivan TJ, Calvi PM Nascimbene R (2013): Towards improved floor spectra estimates for seismic design. *Earthquakes and Structures*, **4**(1), 109-132.

[20] Vukobratović V, Fajfar P (2017): Code-oriented floor acceleration spectra for building structures. *Bulletin of Earthquake Engineering*, **15**, 3013-3026.

[21] Merino R, Perrone D, Filiatrault A (2019): Consistent floor response spectra for performance-based seismic design of non-structural elements. *Earthquake Engineering & Structural Dynamics*, DOI: https://doi.org/10.1002/eqe.3236.

[22] Filiatrault A, Tremblay R, Christopoulos C, Folz B, Pettinga D (2013) *Elements of earthquake engineering and structural dynamics - third Edition*, Polytechnic International Press, Montreal, Canada, 874 pp.

[23] Perrone D, Filiatrault A, Peloso S, Brunesi E, Beiter C, Piccinin R (2019): Experimental seismic response evaluation of suspended piping restraint installations. *Bulletin of Earthquake Engineering*. doi:10.1007/s10518-019-00755-5.

[24] FEMA (2007): *Interim testing protocols for determining the seismic performance characteristics of structural and nonstructural components.* FEMA 461, Federal Emergency Management Agency, Washington DC, USA.

[25] Mazzoni S, McKenna F, Scott MH, Fenves GL (2006): *OpenSees Command language manual*. Pacific Earthquake Engineering Research Center, Berkeley, California.

[26] Lowes LN, Mitra N, Altoontash A (2004): A beam-column joint model for simulating the earthquake response of reinforced concrete frames. *PEER Report 2003/10*. Pacific Earthquake Engineering Research Center, University of California Berkeley, USA.

[27] FEMA (2011): *Quantification of building seismic performance factors: component equivalency methodology*. FEMA P-795. Federal Emergency Management Agency, Washington DC, USA.

